

Multiple locations of boron atoms in the exohedral and endohedral C₆₀ fullereneA. V. Bibikov,^{1,2} A. V. Nikolaev^{1,2,3}, I. V. Bodrenko,⁴ P. V. Borisyyuk,² and E. V. Tkalya^{5,2,6}¹*Skobeltsyn Institute of Nuclear Physics Lomonosov Moscow State University, 119991 Moscow, Russia*²*National Research Nuclear University MEPhI, Kashirskoe shosse 31, 115409 Moscow, Russia*³*School of Electronics, Photonics and Molecular Physics, Moscow Institute of Physics and Technology, 141700 Dolgoprudny, Moscow region, Russia*⁴*CNR/IOM - Cagliari, Cittadella Universitaria di Monserrato, SP Monserrato-Sestu Km 0.700, I-09042 Monserrato, Italy*⁵*P. N. Lebedev Physical Institute of the Russian Academy of Sciences, 53 Leninskiy pr., 119991 Moscow, Russia*⁶*Nuclear Safety Institute of RAS, Bol'shaya Tulsкая 52, 115191 Moscow, Russia*

(Received 23 August 2021; revised 26 November 2021; accepted 3 February 2022; published 18 February 2022)

We study theoretically the bound states of one and two boron atoms in the exohedral and endohedral C₆₀ fullerene. The optimal position of one boron atom is found above the midpoint of the C₆₀ double bond in the exohedral complex, and at the center of C₆₀ or below a carbon atom in the endohedral complex. However, the optimal position of a boron atom is often altered when the second boron atom is added to the molecular complex. For two boron atoms outside the cage the optimal arrangement is realized when the B₂ molecule is attached by one boron atom to a double bond midpoint of C₆₀ or when two boron atoms are above two double bond midpoints on opposite sides of C₆₀. Two endohedral boron atoms can lie on the line joining either two opposite double bond midpoints or two centers of opposite pentagons. The latter case corresponds to the optimal geometry of the B₂@C₆₀ complex provided that two boron atoms are close enough to form the B₂ molecule. In case one boron atom is inside while the other is outside the cage, the optimal locations of atoms are above and below two neighboring carbon atoms belonging to the same hexagon of C₆₀. Remarkably, all these optimal arrangements have different spin states: in the exohedral complex B₂C₆₀ $S = 1$, in the endohedral B₂@C₆₀ $S = 2$ (as in the isolated B₂ molecule), whereas for one boron atom inside and the other outside the cage $S = 0$. The effective (Bader) charge of boron in these configurations varies appreciably—from 0.06e at the center of C₆₀ to 2e in the B₂C₅₈ molecule with two boron atoms substituting for two carbon atoms in C₆₀. We also discuss various conformations in the exohedral and endohedral molecular complexes.

DOI: [10.1103/PhysRevA.105.022813](https://doi.org/10.1103/PhysRevA.105.022813)**I. INTRODUCTION**

The research of endohedral fullerenes with the modern methods of quantum chemistry has become a separate field of investigation [1]. Recently, a vast number of molecular complexes of the type A@C₆₀, where A is an element or a molecule encapsulated into the interior space of the fullerene cage, has been studied theoretically within this approach [1–4]. The progress reached in the field is essential. On the one hand, a fast improvement of the quantum chemistry codes and development of powerful computer clusters allow us to calculate the parameters of nano-objects composed of dozens of atoms with improved accuracy for a reasonable amount of time. On the other hand, we speak here of novel materials, which have not been known before and, therefore, whose physics and chemistry quite naturally draw the attention of many researchers from different fields. Such advanced materials due to their unusual properties can be required and applied in various fields of materials science, physics, chemistry, engineering, and biology [5,9].

In the present work we study the fullerene complexes with boron, where boron can be in the endohedral position—B@C₆₀, B₂@C₆₀—and in the exohedral one—B-C₆₀ and B₂-C₆₀. In addition to the general scientific interest comprising such topics as charge transfer, spin states, and possible

magnetic properties, these molecules can be used in several specific applications, for example, in oncology treatment [5]. The idea of using neutron capture induced decay of ¹⁰B(¹⁰B(n, α)⁷Li) to produce, locally in a tissue, 2.3-MeV α particles for the radiation therapy has a long history [6–8]. Recently, with the development of high-current accelerators for compact neutron sources, the boron neutron capture therapy (BNCT) received a new wave of strong practical interest for clinical applications. Still, one of the challenges in BNCT is the necessity of new boron-containing compounds which can be selectively accumulated in the specific tissues providing sufficient concentration of ¹⁰B. Historically, there are only two drugs that currently are being used clinically, sodium borocaptate (BSH) and boronophenylalanine (BPA) [8], which are far from ideal for many cases. Using a fullerene cage for one or several boron atoms, which can then be functionalized for solubility and vectorized for selective accumulation in target tissues, may be an interesting option for new radio-pharmaceuticals providing the increased nuclide concentration for BNCT.

There is yet another possibility. Upon the interaction of ¹⁰B with protons of the energy exceeding approximately 100 eV, the nuclear reaction ¹⁰B(p, α)⁷Be results in the appearance of ⁷Be. The ⁷Be nucleus as well as ¹⁰B has a very large

TABLE I. Main calculated parameters: binding energy (E_b , in eV), two smallest B-C bond lengths (d_1, d_2 , in Å), the B-B bond length [$d(\text{B-B})$, in Å] in the case when two B atoms are close, average radius (R_{C60}) of C_{60} [Eq. (1), in Å] and its deviation δR_{C60} [Eq. (2), in Å], and Bader charges of boron (in e) for the considered cases. B(in) and B(out) are the number of boron atoms located inside and outside the C_{60} molecular cage. The case “2, 0(mol)” and “0, 2 (mol)” refer to the B_2 molecule located inside and outside C_{60} , respectively, B_2C_{58} to the case where two boron atoms substitute for two carbon atoms of the C_{60} fullerene (E_b in that case is the binding energy of the fullerene). The Bader charge of B indicated by (c) in “2, 0 (mol)” refers to the central atom, indicated by (o) in “0, 2 (mol)” to the outer atom.

B (in,out)	Figure	S	$d_1(\text{B-C})$	$d_2(\text{B-C})$	$d(\text{B-B})$	$\langle R_{C60} \rangle$	δR_{C60}	$Q(\text{B})$	E_b (HF/MP2)
1, 0	1, center	1/2	3.529	3.534		3.531	0.0	0.061	0.405/−0.390
1, 0	2	1/2	1.819	2.210		3.536	0.038	0.586	2.331/0.529
2, 0 (mol)	3	1	1.633	2.249	1.544	3.540	0.041	0.261	1.002/−2.022
								0.610(c)	
2, 0	4(a),(b)	0	2.121	2.158	3.074	3.542	0.018	0.542	4.847/−2.645
2, 0	4(c),(d)	0	2.005	2.349	3.132	3.543	0.015	0.559	4.760/−2.567
2, 0 (mol)	4(e),(f)	2	2.878	2.878	1.474	3.535	0.011	0.601	−1.253/−3.099
0, 1	5(a)–(c)	1/2	1.541	2.720		3.539	0.051	1.299	−1.375/−1.848
0, 1	5(d)–(f)	1/2	1.384	1.467		3.557	0.125	1.800	−0.242/−1.241
1, 1	6	0	1.742	2.228	(in)	3.537	0.057	0.660	0.036/−3.711
			1.606	2.648	(out)			0.760	
0, 2 (mol)	7(a),(b)	1	1.558	2.731	1.584	3.537	0.045	1.228	−4.651/−5.511
								0.034(o)	
0, 2	7(c),(d)	1	1.540	2.720	10.024	3.548	0.075	1.301	−2.725/−3.663
0, 2	7(e),(f)	1	1.626	2.573	10.692	3.541	0.058	0.752	−0.666/−1.361
B_2C_{58} (subs)	8	1	1.531	1.549	7.280	3.552	0.051	1.998	−279.878/−383.814
B_2C_{58} (subs)	8	0	1.532	1.546	7.222	3.598	0.042	2.006	−279.561/−384.386

cross section of the interaction with slow neutrons [10], and therefore, it can also be used for the cancer neutron capturing therapy [11]. However, beryllium is a very toxic chemical, and the C_{60} fullerene is a natural protecting shell for the delivery of ^7Be to tumor sites. In addition, ^7Be is radioactive with the lifetime of approximately 52–53 days [12–15]. Thus, the production of ^7Be in the C_{60} interior region from nonradioactive ^{10}B with the above-mentioned nuclear reaction immediately before the injection of the material into organism offers a

radical simplification of the technological chain for the use of ^7Be in medicine.

For these purposes and for other applications one needs understanding of energy and structural properties of boron atoms located inside and outside the C_{60} fullerene, which is the main goal of the present work. It should be noted that the B_2 molecule differs from other homonuclear diatomic molecules in that it has the spin quintet ($S = 2$) ground state [16,17]. Therefore, for the $B_2@C_{60}$ and B_2C_{60} fullerenes we

TABLE II. The energy E_{1s} of the $1s$ orbital of boron for various complexes and the energy shifts $\Delta E_{1s}^{(1)}$ and $\Delta E_{1s}^{(2)}$ with respect to reference values of $E_{1s}(\text{B})$ (for the isolated boron atom) and $E_{1s}(\text{B}_2)$ (the B_2 molecule), in eV (see text for details). The notations for the first column are as in Table I. Inequivalent B atoms are marked by (1), (2), etc., where (1) refers to the boron atom close to the center, (2) to B close to the cage, (1') to B attached to C_{60} , and (2') to a more distant B.

B (in,out)	Figure	E_{1s}	$\Delta E_{1s}^{(1)}$	$\Delta E_{1s}^{(2)}$
1, 0	1, center	−208.611	0.294	−1.905
1, 0	2	−210.262	−1.358	−3.557
2, 0 (mol)	3	−207.321 (1)	1.584	−0.615
		−208.358 (2)	0.547	−1.652
2, 0	4(a),(b)	−211.305	−2.400	−4.599
2, 0	4(c),(d)	−207.977	0.928	−1.271
2, 0 (mol)	4(e),(f)	−206.071	2.834	0.635
0, 1	5(a)–(c)	−208.837	0.068	−2.131
0, 1	5(d)–(f)	−208.671	0.234	−1.965
1, 1	6	−209.694 (in)	−0.789	−2.988
		−208.858 (out)	0.046	−2.152
0, 2 (mol)	7(a),(b)	−207.977 (1')	0.928	−1.271
		−208.186 (2')	0.718	−1.480
0, 2	7(c),(d)	−208.739	0.166	−2.033
0, 2	7(e),(f)	−209.149	−0.245	−2.444
B_2C_{58} ($S = 1$)	8	−207.394	1.510	−0.688
B_2C_{58} ($S = 0$)	8	−207.386	1.518	−0.680

have to consider possibilities of their ground state to have an open electron shell with nonzero spin quantum number ($S = 1$ or 2).

II. METHOD

The molecular geometry optimization calculations have been performed within the *ab initio* Hartree-Fock (HF) method [18,19] by using GAMESS [20] and GAUSSIAN [21] software. The adopted molecular basis sets were 6-31G for carbon and boron. To account for the electronic correlations effects (responsible, e.g., for the weak dispersion forces), at the HF-optimized configurations, we have performed the second-order Møller-Plesset calculations (MP2) [18]. MP2 computations for the closed electron shells (the spin quantum number $S = 0$) have been carried out with GAMESS whereas for the open shells ($S \neq 0$) with GAUSSIAN. In the last case the restricted open-shell Hartree-Fock (ROHF) method has been employed. HF optimal geometries have been cross-checked with both codes.

The binding energy E_b for a single boron atom encapsulated in the C_{60} fullerene has been defined as

$$E_b = E(\text{B}@C_{60}) - E(\text{B}) - E(C_{60}),$$

and analogously for the other cases.

To quantify the deformation of the C_{60} fullerene cage from the ideal shape we introduce two parameters:

$$\langle R_{C_{60}} \rangle = \frac{1}{60} \sum_a |\vec{r}_a|, \quad (1)$$

$$\delta R_{C_{60}} = \sqrt{\frac{1}{60} \sum_a (|\vec{r}_a| - \langle R_{C_{60}} \rangle)^2}. \quad (2)$$

Here $\langle R_{C_{60}} \rangle$ describes the average radius of the C_{60} fullerene, while $\delta R_{C_{60}}$ is an average displacement of carbon atoms from $\langle R_{C_{60}} \rangle$. For the pristine C_{60} molecule $\langle R_{C_{60}} \rangle = 3.55 \text{ \AA}$ from experimental measurements [22,23] and 3.53 \AA according to the HF calculation with the 6-31G basis, whereas $\delta R = 0$.

Estimations of the effect of temperature on the energies of $\text{B}_n@C_{60}$ bound states due to the motion of atoms in the adiabatic approximation have shown that the influence of zero-point (ZP) vibrations and the thermal motions at temperature $T = 300 \text{ K}$ is negligible. Within the harmonic approximation the ZP vibrational energy of the complexes is about 0.5 Hartree and comes mainly from the vibrations of C_{60} . The difference of the ZP energy values among different bound complexes is less than 0.1 eV. At $T = 300 \text{ K}$ the internal thermal energy is about 0.02 Hartree higher than the ZP energy [21]. The resulting difference in the bound state energies due to the thermal effects is less than 0.01 eV. Therefore, one can safely use the ground-state electron energies for the characterization of the complexes.

III. RESULTS AND DISCUSSION

Although the C_{60} molecule has a very high icosahedral (I_h) symmetry, not all its bonds are equivalent. One distinguishes 30 double bonds and 60 single bonds. Double bonds fusing two neighboring six-carbon rings (hexagons) are stronger and have smaller C-C bond length (l_{db}). Single bonds (with

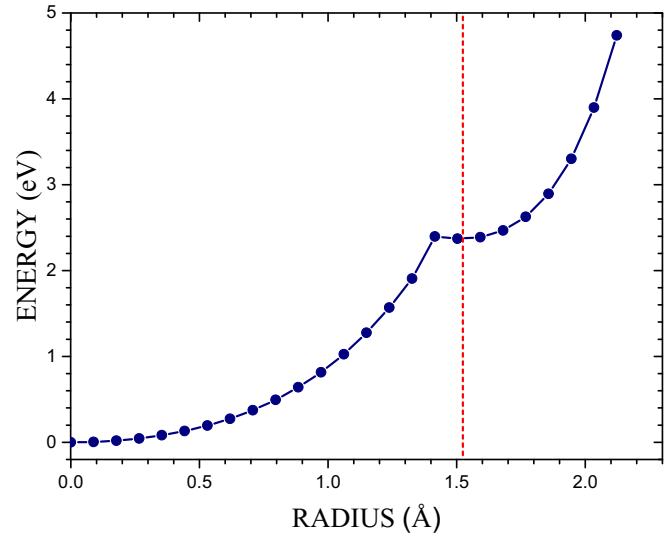


FIG. 1. Two energy minima for the boron atom encapsulated inside the C_{60} fullerene. The energy dependence E (eV) vs radius R in the direction from the center towards any carbon atom of C_{60} , $E(R = 0) = 0$.

$l_{sb} > l_{db}$) form edges of the five-carbon rings (pentagons). Experimentally, $l_{db} = 1.400(15) \text{ \AA}$, $l_{sb} = 1.450(15) \text{ \AA}$ from ^{13}C nuclear magnetic resonance (^{13}C NMR) measurements [22], and $l_{db} = 1.404(10) \text{ \AA}$, $l_{sb} = 1.448(10) \text{ \AA}$ from high resolution neutral scattering [23], with the 3.55-\AA molecular radius ($R_{C_{60}}$). Our calculations with the 6-31G basis set yield $l_{db} = 1.375 \text{ \AA}$, $l_{sb} = 1.452 \text{ \AA}$, and $R_{C_{60}} = 3.530 \text{ \AA}$.

In the following we consider the case of one or two boron atoms (in some cases in the form of the B_2 molecule) attached to C_{60} aiming to study the fullerene as a drug vector delivering boron for medical purposes. Since these atoms can be located inside and outside of the C_{60} molecule, we distinguish several cases. It is worth mentioning that currently only the position of boron at the center of the C_{60} fullerene has been reported in Ref. [24]. The results of our calculations are summarized in Table I with optimal geometries visualized below in Figs. 2–8. Bader charges [25] (BC) in Table I and below are calculated with the MULTIWFN code [26] using the electron density constructed from HF wave functions.

Inside the fullerene the boron atom can be at its center [24]; below a carbon atom, Fig. 2; below the midpoint of double bond, Figs. 3 and 4(c), 4(d); or below the center of a pentagon,

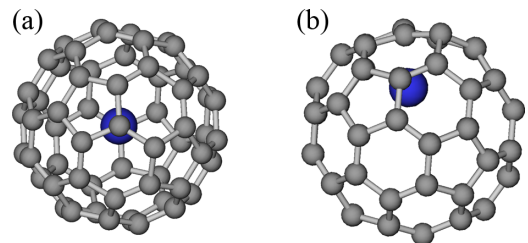


FIG. 2. The secondary optimal geometry for a single boron atom (blue) encapsulated inside C_{60} ($\text{B}@C_{60}$). The boron atom is located on the radius from the center to a carbon atom at 1.82 \AA beneath it.

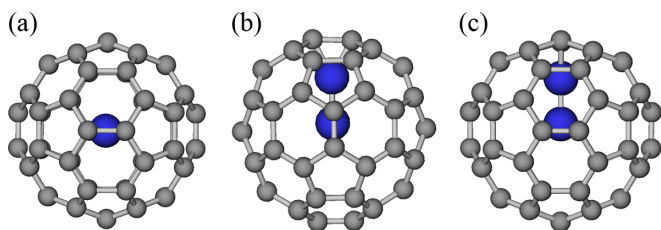


FIG. 3. Two boron atoms encapsulated inside the C_{60} fullerene shown in three different projections. The boron atoms lie on the line joining the center and the double bond midpoint.

Figs. 4(a), 4(b) and 4(e), 4(f). Being outside C_{60} , it can be located above the midpoint of double bond, Fig. 5, or above one of the carbon atoms of C_{60} , Figs. 6 and 7(e), 7(f). Below we consider these cases in more detail.

In addition, since the shifts in the energy E_{1s} of the $1s$ orbital of boron due to a different chemical environment in various states of the exohedral B_nC_{60} and endohedral $B_n@C_{60}$ fullerenes ($n = 1, 2$) could be detectable experimentally in the photon or electron impact spectroscopy, we list them in Table II. One may refer to these numbers as estimates of the ionization energies, when the electron vacancy remains in the $1s$ state of boron. The corresponding values for an isolated B atom and a B_2 molecule are $E_{1s}(B) = -208.905$ eV and $E_{1s}(B_2) = -206.706$ eV, respectively, and for completeness

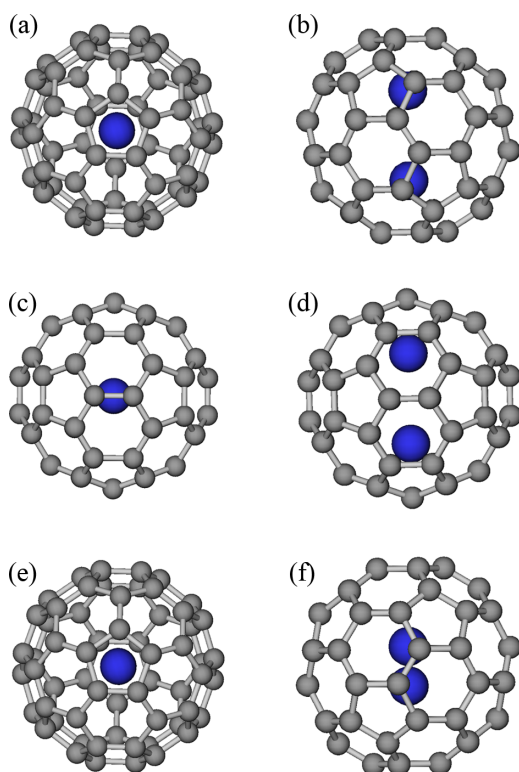


FIG. 4. Three optimal geometries of two boron atoms (blue) encapsulated inside the C_{60} fullerene. (a) and (b) Two boron atoms lie on the line connecting the centers of two opposite pentagons of C_{60} ; (c) and (d) two boron atoms lie on the line connecting the centers of two opposite double bonds; (e) and (f) the B_2 molecule lying on the line connecting the centers of two opposite pentagons.

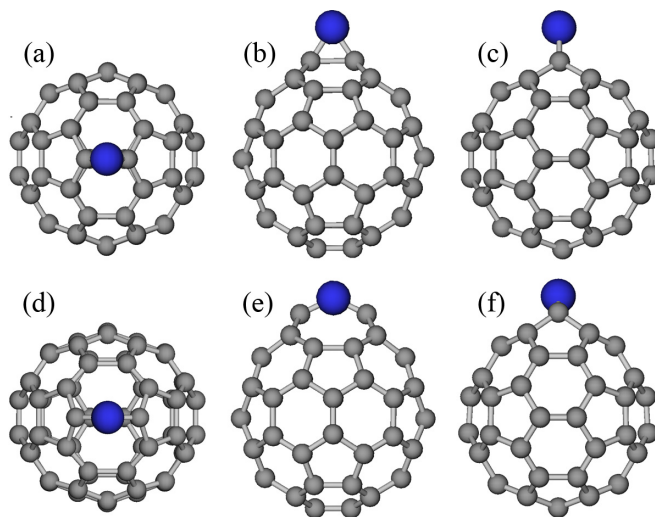


FIG. 5. Two optimal geometries of a single boron atom (blue) located outside the C_{60} fullerene: (1) (a)–(c) different projections corresponding to the conformation with a lower energy; (2) (d)–(f) correspond to the conformation lying 1.188 eV higher in energy in comparison with (1). The boron atom in (2) is closer to the two nearest carbon atoms of C_{60} .

in Table II we also quote energy differences $\Delta E_{1s}^{(1)} = E_{1s} - E_{1s}(B)$ and $\Delta E_{1s}^{(2)} = E_{1s} - E_{1s}(B_2)$ with respect to these reference values. Due to the restricted basis set, nonzero spin (open shell system), and the effect of the electronic correlations, we cannot expect that our absolute values are exact. Nevertheless, these results could guide future experiments of these compounds.

A. One and two boron atoms encapsulated inside C_{60}

We start with illustrating some important features of our results in a simple example. If we consider a single boron atom encapsulated in the C_{60} fullerene and find its energy as a function of boron distance from the fullerene center along the line leading to a carbon atom, we arrive at Fig. 1. While the global minimum at $R = 0$ has been found earlier in Ref. [24], the second energy minimum at $R = 1.51$ Å is new. In Fig. 1 we kept the fullerene geometry fixed. If we allow for the relaxation of the carbon atomic positions, the energy of the second minimum is lowered further by 0.471 eV. (Here and below unless stated otherwise the HF value is implied.) As a result, it becomes well pronounced and identified as a

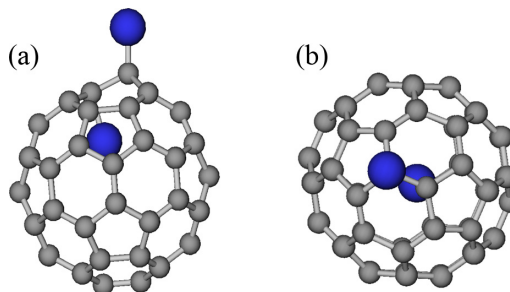


FIG. 6. The optimal geometry for one boron atom inside and one outside the C_{60} fullerene.

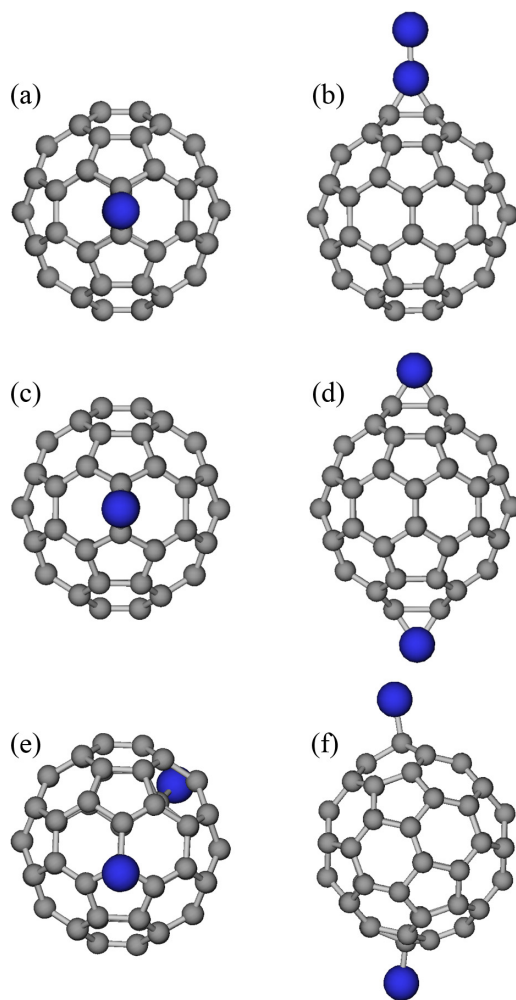


FIG. 7. Optimal geometries of two boron atoms (blue) located outside the C_{60} fullerene: (1) (a) and (b) The B_2 molecule attached by the lower boron atom to two carbon atoms forming the double bond of C_{60} ; (2) (c) and (d) each boron atom is attached to two carbon atoms forming the double bond; (3) (e) and (f) boron atoms are attached to two opposite carbon atoms.

stable minimum in the process of atomic relaxation (Fig. 2). It is worth mentioning that the boron atom resides beneath a carbon atom and therefore its location is different from its boron counterpart put outside the cage which chooses being close to the double bond midpoint (Fig. 5). The effective (Bader) charge of B is that these minima are also different: At the central position it is very small ($0.06e$) whereas in the

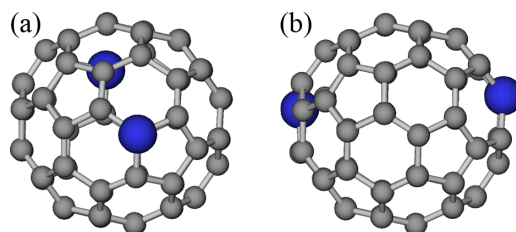


FIG. 8. The optimal geometry of the B_2C_{58} fullerene with two boron atoms substituting for two carbon atoms of the C_{60} molecule.

second minimum it reaches $0.59e$. In comparison with the exohedral molecular complex with one boron atom outside C_{60} [Figs. 5(a)–5(c)] in $B@C_{60}$ the closest B-C bond length (d_1) becomes larger, the second B-C bond length (d_2) smaller (Table I), while the binding energy lies 3.706 eV higher.

If, however, we put two boron atoms inside C_{60} and enable the geometry optimization, the positions of boron atoms are changed: The first becomes displaced from the center and located at $R = 0.281$ Å on the line leading from the center to the double bond midpoint (Fig. 3). The second boron atom lies on the same line at $R = 1.825$ Å. Thus, upon the addition of the second boron atom the optimal positions existing for a single boron atom are transformed to completely new energy minima where even the direction of the line on which both atoms reside is changed. This transformation is accompanied by a sizable redistribution of charge transfer: The charge of the central boron atom changes from $0.06e$ to $0.61e$ while the second boron attached to the fullerene cage becomes less charged ($0.26e$) (Table I). It is also worth mentioning that the ground state of two boron atoms inside C_{60} is the spin triplet with the spin quantum number $S = 1$. The spin singlet state ($S = 0$) lies 0.6304 eV higher.

The boron atomic positions shown in Fig. 3 are asymmetrical in respect to the fullerene center (no inversion symmetry). A close examination indicates that there are also three other different energy minima with symmetrical arrangement of atoms (Fig. 4). These three conformations are shown in (1) Figs. 4(a) and 4(b); (2) Figs. 4(c) and 4(d); and (3) Figs. 4(e) and 4(f). In the cases (1) and (3) two boron atoms lie on the line connecting two centers of opposite pentagons [Figs. 4(a) and 4(e)], and in the case of (2) on the line connecting two centers of opposite double bonds [Fig. 4(c)]. In all these cases the inversion symmetry is conserved, and the former energy minimum associated with the position below the carbon atom, disappears. It is worth noting that while within the HF treatment the energy of (2) is 0.087 eV lower than (1); at the HF+MP2 level the opposite occurs and the energy of (2) becomes 0.078 eV higher than (1).

In the case (3) two boron atoms are in a bound state—they form the B_2 diatomic molecule, which makes the energy of the whole configuration the lowest (Table I). Its energy is 2.255 eV lower than the asymmetrical configuration shown in Fig. 3, and it has a high spin $S = 2$ (quintet) state. The energy difference between the quintet and singlet state reaches 5.926 eV. The spin quintet state of $B_2@C_{60}$ is not completely unexpected because the same spin state occurs in the isolated B_2 molecule [16,17], where the $^5\Sigma_u^-$ ground state lies close in energy to the $^3\Sigma_g^-$ excited level [16]. Apparently, the spin quintet state remains the lowest even when B_2 is encapsulated at the center of the fullerene.

The Bader charge of the boron atoms in going from (1) to (2) and (3) gradually increases from $0.54e$ in (1) to $0.60e$ in (3) (Table I).

B. Single boron atom located outside the C_{60} fullerene

Considering a single boron atom placed outside the C_{60} molecular cage we find two optimal geometries shown in Figs. 5(a)–5(c) and Figs. 5(d)–5(f). The former has lower energy than the latter; the energy difference is 1.133 eV. In both

conformations the boron atom is located above the midpoint of the double bond [Figs. 5(a) and 5(d)], where the concentration of electron density is generally higher than along a single bond. In the second case [Figs. 5(d)–5(f)] the two closest B-C bond lengths d_1 and d_2 become inequivalent ($\Delta d = 0.08$ Å); see Table I. Both of them are smaller than two equivalent B-C bond lengths ($\Delta d = 0$) shown in Fig. 5(b). The boron atom of the configuration in Figs. 5(d)–5(f) virtually pushes aside nearest carbon atoms whose C=C bond length increases from 1.375 Å (in neutral C₆₀) to 2.539 Å [Fig. 5(e)]. This, however, results in a higher total energy in comparison with the first structure where the displacements of carbon atoms are smaller as indicated by smaller radial deviation δR_{C60} . In the first conformation the C=C bond length between double bond carbon atoms remains virtually unchanged (1.373 Å).

The Bader charge of boron is $1.30e$ and $1.80e$ for the first and second configurations, respectively. These values are more than twice as much as effective charges of endohedral boron atoms considered in Sec. III A. These positive charges are largely compensated by negative charges of two carbon atoms connected with the boron atom. The sum of two negative carbon charges is $-1.27e$ for the first configuration and $-1.76e$ for the second.

C. Two boron atoms: one is inside and one is outside C₆₀

With one boron atom inside and one outside the C₆₀ molecular cage one may expect to obtain a combination of the optimal positions found earlier for one boron atom in Figs. 2 and 5. However, this does not occur. While the boron atom inside C₆₀ keeps being under the carbon atom C1, the second boron atom outside the cage changes its position to the one located above another carbon atom C2, which is the nearest neighbor for C1. A close examination shows that C1 and C2 are connected via the double bond and belong to the same hexagon of C₆₀. The boron atom attached to C1 from inside has a larger bond length d_1 but smaller d_2 in comparison with the second boron atom attached to C2 from outside (Table I).

Here we encounter the situation when the addition of a second boron atom forces the first atom to change its optimal location with respect to the fullerene cage. Other examples of this effect are given in Secs. III A and III D. The positive charge of boron atoms located inside and outside the cage ($0.66e$ and $0.76e$) is partially compensated by negative charges of adjacent carbon atoms ($-0.57e$ and $-0.65e$), whereas charges of the other carbon atoms are very small.

We finally note that here the ground spin state is singlet ($S = 0$) in contrast to the optimal cases of two boron atoms put inside ($S = 2$) and outside ($S = 1$) the fullerene cage. We conclude that the electron exchange between two boron atoms, which goes via the electron states of C₆₀, favors the antiferromagnetic arrangements of spins on boron atoms.

D. Two boron atoms outside C₆₀

In case two boron atoms are put outside the C₆₀ molecular cage, three optimal arrangements are found—(1), (2), and (3)—shown in Figs. 7(a) and 7(b); Figs. 7(c) and 7(d); and Figs. 7(e) and 7(f), respectively. The lowest HF energy is in (1), the highest in (3); see Table I. The order of these

configurations is not changed if we take into account the MP2 correction.

Remarkably, the lowest energy for configurations (1), (2), and (3) is found for the spin triplet state ($S = 1$). One can expect it for (1) with the B₂ molecules attached to C₆₀ for the isolated B₂ molecule has a high spin state $S = 2$ [16,17]. As discussed earlier, in the B₂ molecule the $S = 2$ ground state competes with the low lying triplet state. In (1) the triplet state prevails, but in other environments it is not necessarily so. Indeed, for the B₂ molecule encapsulated in C₆₀ the ground state is the spin quintet (Sec. III A).

It is completely surprising that the spin triplet state is realized for cases (2) and (3) when two boron atoms are well separated: $d(\text{B-B}) > 10$ Å (Table I). The only explanation for this fact is that the fullerene molecule gets involved in the spin transfer between two distant boron atoms. This mechanism is known as the indirect exchange (or superexchange) [27,28].

In cases (1) and (2) boron bindings are close to that illustrated in Figs. 5(a)–5(c) for a single boron atom. This is confirmed by close bond lengths d_1 and d_2 and the Bader charges of boron for these cases (Table I). It is also worth noting that while in the triplet state ($S = 1$) of (2) the molecule structure has the inversion symmetry, in the singlet state of (2) we find that two boron atoms are not equivalent. In (3) two bondings between both boron atoms and C₆₀ are approximately equivalent. This type of bonding has been also found for the outer boron atom shown in Fig. 6 and discussed in Sec. III C. The bond lengths d_1 and d_2 and the Bader charges for these cases are close but not identical (Table I). It is worth noting that in the configuration (2) and (3) two boron atoms having positive charges [$1.30e$ in (1) and $0.75e$ in (2)], prefer to stay on opposite sides of the fullerene, whereas for the case when one boron atom is put inside and one outside the cage they come close to each other (Fig. 6).

E. Two boron atoms substituted for two carbon atoms in B₂C₅₈

Finally, we mention that the boron atoms can also substitute for carbon atoms in the C₆₀ fullerene (Fig. 8). Due to the acquired positive charge (about $2e$ Table I), the boron atoms are subjected to the Coulomb repulsion and tend to avoid each other. The optimal configuration is reached when they reside on opposite sides of the fullerene, with the bond pattern equivalent for each boron atom. Three nearest B-C bond lengths—1.531 Å, 1.549 Å, 1.551 Å for the $S = 1$ case (1.532 Å, 1.546 Å, 1.559 Å for the $S = 0$ case)—being slightly different, are larger than the initial double and single bonds of C₆₀ and result in local cage buckling. Then the averaged radius of B₂C₅₈ is increased by 0.02 Å for $S = 1$ (0.07 Å for $S = 0$) with the averaged radial atomic displacement $\delta R_{C60} = 0.05$ Å ($\delta R_{C60} = 0.04$ Å); see Table I. Within the HF treatment the ground spin state is triplet implying that the electron exchange via C₆₀ states favors the ferromagnetic arrangements of spins on boron atoms. The MP2 correction, however, makes the spin singlet the ground state.

IV. CONCLUSIONS

We have studied the optimal positions of one and two boron atoms when they are located inside and outside the C₆₀

fullerene cage, calculated their effective (Bader) charges [25], and analyzed their spin states; see Figs. 2–7 and Table I. For a single boron atom the global energy minima are found for its position above the double bond midpoint in the exohedral location [Figs. 5(a)–5(c)] or at the center of the fullerene in the endohedral location. Another local minimum of the endofullerene B@C₆₀ is detected with the boron lying at 1.82 Å below a carbon atom (Fig. 2). For two boron atoms outside the cage, the energy minima correspond to the B₂ molecule attached by one boron to the double bond midpoint [Figs. 7(a) and 7(b)]. Another candidate is that with two boron atoms above two double bond midpoints on opposite sides of C₆₀ shown in Figs. 7(c) and 7(d), which has a higher energy, and also a conformation with two boron atoms above two opposite carbon atoms [Figs. 7(e) and 7(f)]; see Table I. For two boron atoms in the endohedral location, the lowest minimum is found for the B₂ molecule at the center of C₆₀ and oriented along the line connecting two opposite pentagons [Figs. 4(e) and 4(f)]. Other local energy minima for B₂@C₆₀ are realized for symmetrical boron positions shown in Figs. 4(a)–4(d) or for the asymmetrical arrangement of Fig. 3 with boron atoms on the line joining the center with a double bond midpoint. In the case of one atom inside and the other outside the cage, the boron atoms are attached to two neighboring carbon atoms belonging to the same hexagon of the fullerene (Fig. 6). In general, the energy of the molecule complex is lower if one or two boron atoms are located outside the C₆₀ cage in comparison with analogous configurations with one or two boron atoms inside the cage. It is also worth noting that two boron atoms can substitute for carbon atoms of the C₆₀ fullerene (Fig. 8), with larger B–C bond lengths and deformations of the C₆₀ cage. Since there are various conformations of C₆₀ with two boron atoms lying close in energy, the locations of boron atoms can be altered by transferring to them some energy, e.g., through the absorption of laser radiation. The energy absorption changes such molecular characteristics as effective atomic charges, dipole and quadrupole moments, etc. In particular, Bader charges of boron in these configurations can vary from 0.06e (at the center of the fullerene) to 2e for B₂C₆₀ (Fig. 8). Generally, the Bader charges are larger for boron in exohedral complexes. However, large positive Bader charges of boron are found to be partially compensated by negative charges of the neighboring carbon atoms.

We have found that in the endofullerene B@C₆₀ the addition of the second boron atom affects the location of the first (Sec. III A). The same effect occurs also in the exohedral fullerene BC₆₀, when the second boron atom is put inside the cage; see Sec. III C and Fig. 6. This molecular transformation is accompanied by a sizable change of effective charges of boron atoms.

Except for the $S = 0$ ground state found for the molecule shown in Fig. 6, for two boron atoms the lowest energy is reached in a high spin state. In particular, the global minimum in the exohedral fullerene B₂C₆₀ [Figs. 7(a) and 7(b)] is obtained with $S = 1$, in the endohedral fullerene B₂@C₆₀ [Figs. 4(e) and 4(f)] with $S = 2$. In these two cases two boron atoms are so close that they form the B₂ molecule, which has the $S = 2$ spin in the ground state [16,17]. Therefore, in the exohedral location the C₆₀ fullerene influences B₂ in such a way that the triplet spin state becomes energy preferable.

Surprisingly, the triplet ground state also manifests itself in the configuration shown in Figs. 7(c), 7(d), and Figs. 7(e), 7(f) with two distant boron atoms separated by the fullerene molecule. In that case the mechanism of an indirect exchange (or superexchange) between the boron atoms is enabled [27,28], with the fullerene molecule acting as a mediator.

Various endohedral and exohedral locations of boron atoms considered in this study can be distinguished experimentally in the photon or electron impact spectroscopy measuring shifts of the E_{1s} energy of boron. For that purpose we list calculated values of E_{1s} in Table II. Alternatively, they can be probed in the ultrafast processes of photoexcitation [29].

ACKNOWLEDGMENTS

The reported study was funded by bilateral Russian (RFBR)-Italian (CNR) research Projects No. 20-58-7802 (RFBR) and No. CUP: B55F21000620005 (CNR). We acknowledge a CINECA award under the ISCRA initiative (Project No. IsC92_BeNCT-S) for the availability of high performance computing resources and support. Computations have been partially carried out using the equipment of the shared research facilities of HPC computing resources at Lomonosov Moscow State University [30].

-
- [1] *Handbook of Nanophysics. Clusters and Fullerenes*, edited by K. D. Sattler (CRC Press, Taylor & Francis Group, London, 2011).
- [2] A. A. Popov, S. Yang, and L. Dunsch, *Chem. Rev.* **113**, 5989 (2013).
- [3] H. Shinohara and N. Tagmatarchis, *Endohedral Metallofullerenes: Fullerenes with Metal Inside* (John Wiley & Sons, New York, 2015).
- [4] *Endohedral Fullerenes: Electron Transfer and Spin*, edited by A. A. Popov (Springer, Berlin, Heidelberg, 2017).
- [5] *Medicinal Chemistry and Pharmacological Potential of Fullerenes and Carbon Nanotubes*, edited by F. Cataldo and T. da Ros (Springer, Berlin, Heidelberg, 2008).
- [6] G. L. Locher, *Am. J. Roentgenol., Radium Ther.* **36**, 1 (1936).
- [7] L. E. Farr, W. H. Sweet, H. B. Locksley, and J. S. Robertson, *Transactions of the American Neurological Association (79th Meeting)* **13**, 110 (1954).
- [8] R. F. Barth and J. C. Grecula, *Appl. Radiat. Isot.* **160**, 109029 (2020).
- [9] *Endohedral Metallofullerenes. Basics and Applications*, edited by X. Lu, L. Echegoyen, A. L. Balch, S. Nagase, and T. Akasaka (CRC Press, Boca Raton, 2014).
- [10] T. Rauscher and G. Raimann, *Phys. Rev. C* **53**, 2496 (1996).
- [11] M. A. Scorciapino, C. Nunes, M. Ceccarelli, E. Tkalya, and I. Bodrenko, *J. Nanosci. Nanotechnol.* **21**, 2939 (2021).
- [12] T. Ohtsuki, H. Yuki, M. Muto, J. Kasagi, and K. Ohno, *Phys. Rev. Lett.* **93**, 112501 (2004).

- [13] E. V. Tkalya, A. V. Bibikov, and I. V. Bodrenko, *Phys. Rev. C* **81**, 024610 (2010).
- [14] A. V. Bibikov, A. V. Avdeenkov, I. V. Bodrenko, A. V. Nikolaev, and E. V. Tkalya, *Phys. Rev. C* **88**, 034608 (2013).
- [15] A. V. Bibikov, A. V. Nikolaev, and E. V. Tkalya, *Phys. Rev. C* **100**, 064603 (2019).
- [16] C. F. Bender and E. R. Davidson, *J. Chem. Phys.* **46**, 3313 (1967).
- [17] Z. Rashid, J. H. van Lenthe, and R. W. A. Havenith, *Comp. Theor. Chem.* **1116**, 92 (2017).
- [18] A. Szabo and N. S. Ostlund, *Modern Quantum Chemistry* (McGraw-Hill, Dover, 1989).
- [19] A. Artemyev, A. Bibikov, V. Zayets, and I. Bodrenko, *J. Chem. Phys.* **123**, 024103 (2005).
- [20] M. W. Schmidt, K. K. Baldrige, J. A. Boatz, S. T. Elbert, M. S. Gordon, J. H. Jensen, S. Koseki, N. Matsunaga, K. A. Nguyen, S. Su, T. L. Windus, M. Dupuis, and J. A. Montgomery, *J. Comput. Chem.* **14**, 1347 (1993).
- [21] M. J. Frisch, G. W. Trucks, H. B. Schlegel, G. E. Scuseria, M. A. Robb, J. R. Cheeseman, G. Scalmani, V. Barone, G. A. Petersson, H. Nakatsuji, X. Li, M. Caricato, A. V. Marenich, J. Bloino, B. G. Janesko, R. Gomperts, B. Mennucci, H. P. Hratchian, J. V. Ortiz, A. F. Izmaylov, J. L. Sonnenberg, D. Williams-Young, F. Ding, F. Lipparini, F. Egidi, J. Goings, B. Peng, A. Petrone, T. Henderson, D. Ranasinghe, V. G. Zakrzewski, J. Gao, N. Rega, G. Zheng, W. Liang, M. Hada, M. Ehara, K. Toyota, R. Fukuda, J. Hasegawa, M. Ishida, T. Nakajima, Y. Honda, O. Kitao, H. Nakai, T. Vreven, K. Throssell, J. A. Montgomery, Jr., J. E. Peralta, F. Ogliaro, M. J. Bearpark, J. J. Heyd, E. N. Brothers, K. N. Kudin, V. N. Staroverov, T. A. Keith, R. Kobayashi, J. Normand, K. Raghavachari, A. P. Rendell, J. C. Burant, S. S. Iyengar, J. Tomasi, M. Cossi, J. M. Millam, M. Klene, C. Adamo, R. Cammi, J. W. Ochterski, R. L. Martin, K. Morokuma, O. Farkas, J. B. Foresman, and D. J. Fox, *Computer code GAUSSIAN 16, Revision C.01* (Gaussian, Wallingford, 2016).
- [22] W. I. F. David, R. M. Ibberson, J. C. Matthewman, K. Prassides, T. J. S. Dennis, J. P. Hare, H. W. Kroto, and D. R. M. Walton, *Nature (London)* **353**, 147 (1991).
- [23] K. Prassides, H. W. Kroto, R. Taylor, D. R. M. Walton, W. I. F. David, J. Tomkinson, R. C. Haddon, M. J. Rosseinsky, and D. W. Murphy, *Carbon* **30**, 1277 (1992).
- [24] Vinit and C. N. Ramachandran, *J. Phys. Chem. A* **121**, 1708 (2017).
- [25] R. F. W. Bader, *Atoms in Molecules: A Quantum Theory*, International Series of Monographs on Chemistry (Oxford University Press, Oxford, New York, 1994).
- [26] T. Lu and F. Chen, *J. Comput. Chem.* **33**, 580 (2012).
- [27] P. W. Anderson, *Phys. Rev.* **79**, 350 (1950).
- [28] A. V. Nikolaev and K. H. Michel, *J. Chem. Phys.* **122**, 064310 (2005).
- [29] M. El-Amine Madjet, E. Ali, M. Carignano, O. Vendrell, and H. S. Chakraborty, *Phys. Rev. Lett.* **126**, 183002 (2021).
- [30] V. Sadovnichy, A. Tikhonravov, V. Voevodin, and V. Opanasenko, in *Contemporary High Performance Computing: From Petascale Toward Exascale*, Chapman & Hall/CRC Computational Science (CRC Press, Boca Raton, 2013), p. 283.